Cinnamomi ramulus exhibits anti-proliferative and anti-migration effects on MH7A rheumatoid arthritis-derived fibroblast-like synoviocytes through induction of apoptosis & cell arrest and suppression of matrix metalloproteinase

Jia Liu
School of Pharmacy, Chengdu University of Traditional Chinese Medicine, Chengdu 611130, P.R. China. Chengdu Institute for Food and Drug Control, Chengdu 611137, P.R. China
Qing Zhang
School of Pharmacy, Chengdu University of Traditional Chinese Medicine, Chengdu 611130, P.R. China
Ruo-Lan Li
School of Pharmacy, Chengdu University of Traditional Chinese Medicine, Chengdu 611130, P.R. China
Shu-Jun Wei
School of Basic Medicine, Chengdu University of Traditional Chinese Medicine, Chengdu 611130, P.R. China
Yong-Xiang Gao
School of Basic Medicine, Chengdu University of Traditional Chinese Medicine, Chengdu 611130, P.R. China
Wei Jin
Emergency Department, Hospital of Chengdu University of Traditional Chinese Medicine, Chengdu 610072, P.R. China
Chun-Jie Wu
School of Pharmacy, Chengdu University of Traditional Chinese Medicine, Chengdu 611130, P.R. China
Xufeng Pu (pxf68@263.net)
Chengdu University of Traditional Chinese Medicine

Research

Keywords: Cinnamomi ramulus, Rheumatoid arthritis, Apoptosis, Cell cycle, Synovial fibroblasts, Anti-arthritic effect, MH7A

Posted Date: February 24th, 2020

DOI: https://doi.org/10.21203/rs.2.24246/v1

Abstract

Background: Rheumatoid arthritis (RA) is a complex chronic inflammatory disease that is associated with the aberrant activation of fibroblast-like synoviocytes (FLS). The extract of *Cinnamomi ramulus* has been reported to exert alleviates pain, anti-tumor and anti-inflammatory effects. The present study was designed to investigate the effects of *Cinnamomi ramulus* on RA and explore the underlying mechanisms.

Material/methods: TNF-α induced human synoviocyte MH7A cells was performed to evaluate the anti-proliferative and anti-migration effect of *Cinnamomi ramulus*. The anti-proliferative effect of *Cinnamomi ramulus* was determined by CCK-8 assay and colony formation assay. Apoptosis was measured by AnnexinV FITC/PI staining and flow cytometry. Cell cycle was evaluated by flow cytometry. The expressions of mitochondrial apoptosis and cell cycle-related molecules, including Bcl-2, Bax, C-Caspase-3, CDC2 and Cycylin B1 were determined by Western blotting. Furthermore, the migration and invasion abilities of MH7A cells were determined using scratch wound healing assay and transwell assay. mRNA expressions of (MMP)-1, -2, & -3, P53, P21 and Cyclin D were determined using qRT-PCR analysis. For qualitative analysis on its chemical components, an ultra-high performance liquid chromatography (UPLC) coupled with Q-Exactive MS (QE-MS) was established for rapid separation and structural identification of the constituents in *Cinnamomi ramulus*. The further computationally study on the relationships between the 9 compounds and the potential target proteins of RA were carried out with molecular docking strategy.

Results: Our data demonstrate that *Cinnamomi ramulus* inhibited proliferation of MH7A cells, induced cell apoptosis, blocked the cell cycle in the G2/M phase and regulated the protein expression of Bcl-2, Bax, C-Caspase-3, CDCD2 and Cyclin B1. Moreover, *Cinnamomi ramulus* was proven to significantly inhabited migration and invasion of MH7A cells through inhibition of levels of matrix metalloproteinase (MMP)-1, -2, & -3.*Cinnamomi ramulus* reduced mRNA levels of CDK4 whereas increased the expression of P53, P21 and CyclinD, implying its regulation effects on apoptosis and cell cycle distribution in MH7A cells. The chromatographic profiling of the extract by UPLC-QE-MS/MS analysis showed 9 compounds are the main components. And the molecular docking strategy results showed that the compounds in *Cinnamomi ramulus* have good affinity with protein crystal, and benzyl cinnamate may be the main active component of *Cinnamomi ramulus* to induce cell apoptosis and cycle resistance.

Conclusions: *Cinnamomi ramulus* exhibits anti-proliferative and anti-migration effects on MH7A rheumatoid arthritis-derived fibroblast-like synoviocytes through induction of apoptosis & cell arrest and suppression of matrix metalloproteinase.

Background

RA is a chronic autoimmune joint disease characterized by synovial tissue inflammation, destruction of articular cartilage, and deformities of the joints whose exact cause is still not completely known [1, 2].

Synovial fibroblasts (SFs) play an important role in cartilage destruction by mediating most relevant pathways. Increasing evidences have suggested that activated synovial fibroblasts can manifest similar properties of tumor-like cells, such as hyperproliferation and insufficient apoptosis [3]. The uncontrolled proliferation of synovial fibroblasts has been thought to contribute to the formation of rheumatoid arthritis (RA) [4]. Meanwhile, Synovial fibroblasts also can spontaneously secrete numerous pro-inflammatory cytokines and matrix metalloproteinases (MMPs), which plays an important role in progressive destruction of articular cartilage [5, 6]. Thus, that promoting apoptosis and inhibiting proliferation of synovial fibroblasts is believed to exert potential therapeutic effects on RA.

Cinnamomi ramulus, known as “Guizhi” in China and “Geiji” in Korea, has been traditionally used to reduce chronic joint pain in patients with arthritis [7, 8]. it’s reported that the extract of Cinnamomi ramulus has a variety of biological activities, including analgesic, anti-tumor and anti-inflammatory activities [9, 10]. These bioactivities of Cinnamomi ramulus might be depend on the presence of certain classes of compounds in this plant, such as phenylpropanoids, monoterpenoids, sesquiterpenoids, sterols, etc [11]. Although therapeutic potentials of Cinnamomi ramulus for inflammatory reactions have been investigated, its effect in RA is currently poorly understood. In previous studies, we found that the traditional Chinese recipe guizhi-shaoyao-zhimu decoction had a significant anti-arthritic effect [8], and Cinnamomi ramulus one of the most important herbal medicines in this traditional Chinese Medicine (TCM) formula. In addition, there are also many other TCM formulas with good curative effect for RA with Cinnamomi ramulus as the main component, such as huangqi guizhi wuwu decoction, guizhi fuzi decoction, and chai hu guizhi ganjiang decoction, etc [12–14]. In addition, some modern studies have confirmed the anti-RA potential of Cinnamomi ramulus, but the detail molecular mechanisms remains unclear.

In this paper, we assessed the anti-arthritic effects of the aqueous extract of Cinnamomi ramulus on a human synovial fibroblast cell line (MH7A), focusing on possible mechanisms associated with anti-inflammatory, suppressing invasion & migration of synovial fibroblasts, and inducing cell cycle arrest and apoptosis. In addition, we used the molecular docking to study the interactions between the main compounds of Cinnamomi ramulus and the rheumatoid arthritis-associated protein targets. Therefore, our present study provides a direction for the mechanism and drug research of anti-rheumatoid arthritis of Cinnamomi ramulus, as well as a reference for the new treatment strategy of rheumatoid arthritis and the clinical application and development of Cinnamomi ramulus.

Materials And Methods

Reagents and Chemicals

Fetal bovine serum (FBS), phosphate buffered saline (PBS), Penicillin-Streptomycin, trypsin-EDTA and Dulbecco’s modified Eagle medium (DMEM) were purchased from GIBCO (Grand Island, NY, USA). The human TNF-α was purchased from Pepro Tech (Rocky Hill, NJ, USA). Griess reagent, dimethyl sulfoxide (DMSO), Cell Counting Kit-8 (CCK-8 kit), BCA Protein Assay Kit, and Annexin V-FITC/PI apoptosis kits were

purchased from the BOSTER Biol.Tech. Co. (Wuhan, China). Cell Cycle Staining kits were purchased from Beyotime Biotechnology Company (Haimen, China). TRIzol™ Plus RNA Purification Kit (Invitrogen life technology, Carlsbad, CA, USA), ReverTra Ace® qPCR RT Master Mix (Beans Biol Tech. Co., Tokyo, Japan) and SYBR Green RT-PCR reaction kit (QPK-201, Toyobo, Tokyo, Japan) were used in RT-PCR experiment.

Cell culture

A human synovial cell line MH7A was purchased from the Beina Biological Company (Beijing, China), and cultured in DMEM medium with 10% FBS at 37 °C in 5% CO_2 humidified atmosphere. Cells were passaged every 3–4 days, and cells obtained from the 5-10th passages were used for the experimental procedures.

Preparation of *Cinnamomi ramulus* extract

For laboratory study, authentic plant materials were purchased from the Neautus Chinese Herbal Pieces Ltd. Co. (Chengdu, China), and were identified by Prof. Chun-Jie Wu (School of Pharmacy, Chengdu University of Traditional Chinese Medicine). Plant material (200 g) was air-dried and cut into small pieces. The prepared sample was soaked by 300 mL of distilled water for 2 h and then left to boil for 1 h in a closed flask. Afterwards, the filtrates were cooled to room temperature and subsequently dried by frozen (-20 °C) and lyophilized to afford the dry extract (0.6678 g). Then, the Cinnamomi ramulus extract (CRE) was dissolved in DMEM at the appropriate concentrations for the further experiment.

Cell viability assay

Cell viability was determined using the CCK-8 kit according to the instruction of manufacturer. Briefly, MH7A cells were seeded at 5×10^3 cells/well in 96-well culture plates in DMEM containing 10% FBS, incubated overnight. Then cells were stimulated with TNF-α (20 ng/mL) and exposed at various concentrations of CRE for 24 h. After that, CCK-8 was added to each well of the plate and incubated at 37 °C for 1.5 h. The resulting optical density was detected at 450 nm by a multi-detection iMARK microplate reader (BIO-RAD, Hercules, CA, USA).

Apoptosis Assay

MH7A cells (5×10^5 cells/well) were seeded onto 6-well plates, and cultured for 12 h. After the incubation, cells were treated with different concentrations CRE (0.4, 0.8, 1.2 mg/mL) and TNF-α (20 ng/mL) for 24 h. After treatment, the cells were harvested and washed with PBS, and subsequently stained with AnnexinV FITC/PI apoptosis assay kit according to the manufacturer's instructions. Afterward, apoptosis was analyzed by laser scanning confocal microscope (Leica TCS SP8 STED, Heidelberg, Germany) and FACS Calibur flow cytometry (Becton Dickinson, San Jose, CA, USA).

Cell Cycle Assay

MH7A cells (5×10^5/well) were inoculated on 6-well plates and cultured for 12 h. Cells were incubated with different concentrations of CRE (0.2, 0.4, 0.6 mg/ml) and TNF-α (20 ng/mL) for 24 h. For analysis of

the cell cycle distribution, the supernatant was discarded, and attached cells were harvested and fixed in cold 75% ethanol. The cells were then kept at -20 °C for 24 h before analysis. Cells were stained with propidium iodide (PI; Sigmar), and the DNA content was determined by FACS Calibur flow cytometry (Becton Dickinson, San Jose, CA, USA) to analyze the cell cycle.

Scratch wound healing experiment

Cell migration assay was performed by wound healing assay. MH7A cells (5×10^5 /well) were seeded into a 6-well plate, and when the cells covered the whole bottom surface of the well, the serum-free medium was used to continue the culture for 12 h, so as to eliminate the influence of normal cell growth on the scratch experimental results. After that, a p200 pipet tip was used to make a scratch at the bottom of the well, and the cells were treated with TNF-α (20 ng/mL) and CRE (0.2, 0.4 and 0.6 mg/mL). After 24 hours of scratch, cells were stained with crystal violet, and an inverted microscope (Nikon TS2, Tokyo, Japan) was used to observe and photograph the scratch area, and then the distance change of the scratch area was measured and analyzed.

Transwell experiment

Transwell chamber was used to assess the migration and invasion capacity of cells. The cells (1×10^5/well) were seeded in a serum-free medium in the upper chamber of transwell (Corning Inc, Corning, NY, USA), and a DMEM medium containing 20% serum in the lower chamber,and cells treated with TNF-α (20 ng/mL) or CRE (0.2, 0.4 and 0.6 mg/mL) for 24 h. After that, the transwell chambers were removed, and the cells inside the membrane were gently scraped off with a cotton swab, while the cells outside the membrane were thought to be migratory or invasive. The migratory or invasive cells were fixed with 4% paraformaldehyde at room temperature for 20 min. Wash with PBS three times and stain with crystal violet for 10 min. Finally, an inverted microscope (Nikon TS2, Tokyo, Japan) was used to observe and photograph. In addition, Image J software (version 1.51, nih, MD) was used to count invasive cells. In contrast to the migration experiment, 0.1% matrigel (BD) was spread at the bottom of the transwell chamber in the invasion experiment.

Colony formation assay

MH7A cells (1×10^3/well) were seeded in 6-well plates and treated with TNF-α (20 ng/mL) and CRE (0.2, 0.4 and 0.6 mg/mL) for 24 h. The cells were cultured in a new medium for a week, the cells were immobilized and stained with crystal violet, the number of colony formation was counted in a random microscopic field and the photos were taken.

Western blot analysis (WB)

MH7A cells (5×10^5/mL) were treated with TNF-α (20 ng/mL) and various concentrations of CRE (0.2, 0.4, 0.6 mg/ml) for 24 h. RIPA lysis buffer (containing protease and phosphatase inhibitors) was used to collect protein from cell samples. The supernatant of lysate was boiled, and total protein was measured using a BCA kit. Proteins were separated by SDS-PAGE, and then transferred to polyvinylidene fluoride (PVDF) membrane. The membranes were blocked with 5% BSA (Bovine SerumAlbumin) in TBST (Tris-

Buffered Saline and Tween 20) at room temperature for 1 h, followed by exposure to the corresponding primary antibodies overnight at 4 °C. After washing with TBST for three times, the membranes were incubated with the secondary antibodies. Proteins were scanned using the ECL detection system, the gel images were analyzed using the Image J (v1.51) image processing software.

RNA extraction and quantitative real-time PCR (qPCR)

According to the manufacturer's instructions, total RNA was extracted using Trizol reagent according to the manufacturer's instructions and each sample was reverse transcribed using the cDNA synthesis kit according to the manufacturer's protocol. The mRNA expressions of MMP-1, 2 & 3, P53, P21, CDK4 and Cyclin D were determined by qRT-PCR assays using SYBR Green PCR Premix Ex Taq II reagents on a Light Cycler 480 II real-time system (Roche, Mannheim, Germany). GAPDH, a house-keeping gene, was used for was used as a quantitative control for RNA levels. Relative gene expression was calculated by the ΔΔCt method. The sequences for the relevant primers are listed in Table 1. qPCR was run with an initial denaturation step at 95 °C for 30 s, followed by extension step at 57 °C and 30 s for 44 cycles.

Table 1
Primer sequences used for quantitative real-time PCR

Target genes	Sequence	
MMP-1	Forward: Reverse:	CTCAATTTCACTTCTGTTTTCTG CATCTCTGTCGGCAAATTCGT
MMP-2	Forward: Reverse:	CGGTGCCCAAGAATAGATG AAAGGAGAAGAGCCTGAAGTG
MMP-3	Forward: Reverse:	GGCTTCAGTACCTTCCCAGG GCAGCAACCAGGAATAGGTT
p53	Forward: Reverse:	CAGCCAAGTCTGTGACTTGCACGTAC CTATGTCGAAAAGTGTTTCTGTCATC
p21	Forward: Reverse:	AGATGTCCAGCCAGCTGCACCTGAC CTATGTCGAAAGTGTTTCTGTCATC
CDK4	Forward: Reverse:	ACGCCTGTGGTGGTTACG CCATCTCTGGCACCACTGAC
Cyclin D	Forward: Reverse:	CAAACAGATCATCCGCAAAC GCGTGTGAGGCGGTAGT
GAPDH	Forward: Reverse:	AGCCACATCGCTCAGACAC GCCCAATACGACCAAATCC

Qualitative UPLC-QE-MS analysis

Thermo Scientific Q Exactive Orbitrap HRMS (Thermo Fisher Scientific, Massachusetts, USA) in conjunction with a Thermo Scientific Vanquish UPLC (Thermo Fisher Scientific, Massachusetts, USA). Chromatographic separation was achieved on an Thermo Scientific™ Accucore™ C18 (3 × 100 mm,

2.6 μm) in a thermostatically controlled column compartment (30 °C). The aqueous and organic mobile phases used were 0.1% formic acid in water (A) and methyl alcohol (B), respectively. A gradient elution system was set up as follows: 0–20 min, 5–80% B; 20–30 min, 80–95% B; 30.1–35 min, 95–5% B. The flow rate was 0.3 mL/min, and 2 μL of the extraction was injected to the LC system. The instrument was operated in positive ion mode to perform full-scan analysis over an m/z range of 100–1500. And the optimized parameters were set as follows: the sheath gas flow rate-35 L/min; spray voltage-3000V; capillary temperature-320V; aux gas flow rate-10.00L/min; max spray current-100A; probe heater temperature-350 °C; S-lens RF level-50.00%.

Molecular docking studies

According to the preliminary analysis by UPLC-QE-MS/MS, Cinnamomi ramulus contained 9 chemical components. Find the structure formula of the compound in PubChem (https://pubchem.ncbi.nlm.nih.gov/), use ChemDraw software (version 14.0, CambridgeSoft, Cambridge, Massachusetts, USA) to draw the structure of the compound and save it as MOL file. Then, according to the previous WB and q-PCR results, Bcl-2, Caspase 3, MMP3, CDC2, Cyclin B1, CDK4, P21, P53 and Cyclin D as the target of the function RA in Cinnamomi ramulus. Human protein complex crystals with prototype small molecular ligands for these targets are downloaded from the PDB (http://www.rcsb.org) website, and the standard name of the target is confirmed by Uniprot (http://www.uniprot.org/). Molecular docking was performed using Discovery studio software (DS, version 4.5.0, Biovea Inc., Omaha, NE, USA) in the same manner as before. In simple terms, the target protein crystal composite and compounds of MOL files are imported into DS software, according to prototype Ligand binding site, using the Ligand Docking module, and using molecular Docking of rigid Docking. A compound with a higher docking score than the prototype ligand is considered as an active compound capable of binding to the target.

Statistical analysis

All results were presented as mean ± standard deviation (SD). Statistical significance between groups was analyzed by Student-t test or ANOVA of SPSS software (version 19). Statistical significance was defined as a $p < 0.05$.

Result

Cinnamomi ramulus extracts inhibits the proliferation of synovial fibroblasts

CCK-8 assay was carried out to examine the cytotoxicity of *Cinnamomi ramulus* extract (CRE) (0.1, 0.2, 0.4, 0.8, 1.0 and 2.0 mg/mL) on TNF-α stimulated MH7A cells. As shown in Fig. 1, it revealed that CRE could inhibit the proliferation of MH7A cells in a concentration-dependent manner.

Furthermore, colony formation is an *in vitro* cell survival assay that is based on the ability of a single cell to grow into a colony. The assay essentially tests every cell in the population for its ability to undergo

“unlimited” division, and to measure the proliferation capacity of the cells [15]. interestingly, similar to the results of CCK-8 assay, colony formation assay showed that CRE (0.2, 0.4 and 0.6 mg/mL) significantly and concentration-dependently inhibited the colony formation rate (P<0.001), compared to the control cells (Fig. 2).

Cinnamomi ramulus extracts induces apoptosis in synovial fibroblasts

In order to determine whether the cytotoxic effects of CRE on MH7A cells are related to induction of apoptosis or not, flow cytometry and laser scanning confocal microscope with AnnexinV FITC/PI staining were used to determine the apoptosis in MH7A cells. As shown in Fig. 3, different concentrations of CRE (0.4, 0.8, 1.2 mg/mL) could significantly induce the apoptosis of MH7A cells (P<0.001), compared to the control group (MH7A cells treated by TNF-α alone). Furthermore, similar to the results of flow cytometry analysis, the MH7A cells treated with CRE (0.4, 0.8, 1.2 mg/mL) were also observed using laser scanning confocal microscope to exhibit early and late apoptotic characteristics (Fig. 4).

Furthermore, we analyzed the effect of CRE on expression of apoptosis-associated proteins by western blotting assays. As shown in Fig.5, the results showed that CRE (0.2, 0.4, 0.6 mg/mL) significantly elevated the expressions of Cleaved (C)-Caspase-3 (P<0.001) and Bax (P<0.001), whereas reduced the expressions of Bcl-2 (P<0.001) in concentration-dependent manner, compared to the control MH7A cells, which was consistent with results from previous apoptosis analysis.

Cinnamomi ramulus extracts induces G2/M phase arrest in synovial fibroblasts

The effect of CRE on cell cycle distribution was studied by flow cytometry analysis. The results showed that CRE (0.2, 0.4, 0.6 mg/mL) treatments resulted in a concentration-dependent increase in the proportion of G2 phase cells, accompanied by a decrease in G1 phase cells (Fig. 6). Therefore, in order to further investigate whether the cell cycle arrest due to the exposure to CRE or not, we examined the relative levels of cell cycle-related genes and proteins after treatment with different concentrations of CRE (0.2, 0.4, 0.6 mg/mL). The experimental results of the Western blotting and q-PCR assays showed that compared with the control MH7A cells, CRE treatment (0.2, 0.4, 0.6 mg/mL) resulted in the up-regulation of Cyclin D (P<0.01), P53 (P<0.01) and P21 (P<0.01), accompanied by the down-regulation of CDK4 (P<0.01), Cyclin B1(P<0.01) and CDC2 (P<0.01) (Fig. 5 & Fig. 7), the results are consistent with the results of G2 cell cycle arrest obtained by flow cytometry, and confirming the involvement of CRE in the regulation of cell cycle. Taken together, these results suggest that CRE treatment can induce G2 phase arrest in MH7A cells.

Cinnamomi ramulus extracts inhibits cell migration and invasion in synovial fibroblasts

The wound healing and transwell assays carried out to determine the cell migration and invasion in MH7A cells, and the results showed that CRE (0.2, 0.4, 0.6 mg/mL) can inhibit cell migration and invasion of MH7A cells with a concentration-dependent manner. In the wound healing assay (Fig. 8A), we found that the scratch prepared by pipette tip in the normal and TNF-α stimulated groups were almost fully filled with MH7A cells, however, the migratory ability of cells in the CRE-treated cells were decreased compared with the control MH7A cells (P<0.001). Similar to the results of wound healing assay, significant decreased cells were detected in CRE (0.2, 0.4, 0.6 mg/mL) treated MH7A cells for the transwell migration experiment (P<0.01), compared to the control MH7A cells (Fig. 8B). Furthermore, transwell chambers with matrigel were used to detect the invasive capacity of MH7A cells. The results showed CRE (0.2, 0.4, 0.6 mg/mL) caused significant suppression of the invasive cells in the Matrigel-Transwell experiment (P<0.001), compared to the control MH7A cells (Fig. 9)

Cell migration and invasion are closely related to matrix degradation, a process mainly dependent on the activities of degradation enzymes such as MMPs [16]. The Quantitative real-time PCR (q-PCR) assays of MMP-1, 2 & 3 were carried out to explore its related molecular mechanism. As shown in Fig. 10, all the testing MMPs (including MMP-1, MMP-2, MMP-3) were significantly increased by TNF-α stimulation (P<0.001), compared to the normal MH7A cells. Interestingly, the increased MMPs could be significantly reduced by CRE (0.2, 0.4, 0.6 mg/mL) (P<0.01) compared to the control MH7A cells. The data mentioned above manifested that CRE could obviously reduce the migration and invasion of TNF-α stimulated MH7A via suppression of MMPs expressions.

Results of the constituents analysis of *Cinnamomi ramulus* extracts by UPLC-QE-MS/MS

UPLC-QE-MS/MS was used to analyze the freeze-dried powder of Cinnamomi ramulus aqueous extracts, as shown in the materials and methods section. Figure 11 showed the MS total ion chromatograms (TIC) provided by analysis of the aqueous extracts in positive ionization modes. To qualitative investigate the main constituents of water extracts of Cinnamomi ramulus, we compared individual retention times (t_R), the online MS spectra and the reference standards in the literature to confirm the identity of the analyte. Peaks 1–9 were unequivocally identified as anisic acid, coumarin, 2-methoxycinnamic acid, coniferyl aldehyde, azelaic acid, cinnamic acid, cinnamaldehyde, 4-methoxy-cinnamaldehyde and benzyl cinnamate, respectively. Reference standards were used to confirm the retention times, accurate mass and fragment ions. Tentatively identified compounds in the aqueous extracts from Cinnamomi ramulus (Fig. 11) and the main parameters that support their identification are presented in Table 2.

Table 2
Chemical constituents identified from the Cinnamomi ramulus extracts

Peak	t_R (min)	Measured mass (m/z)	MS/MS fragments (m/z)	Identification
1	1.32	153.05481 $[M + H]^+$	135, 107, 92, 77	Anisic acid [17]
2	9.72	147.04434 $[M + H]^+$	103, 91, 77, 65	Coumarin [18]
3	12.01	179.07014 $[M + H]^+$	161, 137, 135	2-Methoxycinnamic acid [19]
4	12.39	179.07024 $[M + H]^+$	161, 147, 119, 107, 91, 79, 65	Coniferyl aldehyde [19]
5	13.07	189.09706 $[M + H]^+$	152, 124, 111, 98, 84, 83, 73, 69, 60, 55, 41	Azelaic acid [20]
6	13.89	149.05971 $[M + H]^+$	131, 123, 103	Cinnamic acid [18]
7	15.15	133.06502 $[M + H]^+$	115, 105, 103, 91, 79, 77, 55	Cinnamaldehyde [18]
8	18.08	163.07555 $[M + H]^+$	145, 135, 121, 105, 79, 55	4-Methoxycinnamaldehyde [18]
9	28.84	239.10709 $[M + H]^+$	238, 193, 131, 103, 91, 77, 65	Benzyl cinnamate [21]

Molecular docking study

In order to study the active substance basis of Cinnamomi ramulus for its anti-RA effects, the molecular docking strategy was carried out to screen the identified 9 compounds. The active targets were proteins or genes reported in previous paper, and ultimately nine potential protein targets and their target protein-ligand crystal complexes were downloaded from the PDB (Table 3). The experimental results showed that compound 9 (benzyl cinnamate) had a good affinity with these selected protein targets, and its docking score was much higher than that of the prototype ligand of the target proteins, suggesting that compound 9 might be an important active component of Cinnamomi ramulus for its anti-RA effects. The results are shown in Fig. 12.

Table 3
Information of the 9 potential target proteins investigated in the present study

Uniport ID	PDB ID	Target Protein	Gene
P10415	6RNU	Apoptosis regulator Bcl-2	Bcl-2
P42574	3H0E	Caspase-3	Caspase 3
P14635	4Y72	G2/mitotic-specific cyclin-B1	Cyclin B1
P24385	6GUB	G1/S-specific cyclin-D1	Cyclin D
P38936	5XVA	Cyclin-dependent kinase inhibitor 1	P21
P04637	6ET4	Cellular tumor antigen p53	P53
P11802	1H00	Cyclin-dependent kinase 4	CDK 4
P06493	6FT8	Cyclin-dependent kinase 1	CDC 2
A5GZ70	1D5J	Matrix metalloproteinase 3	MMP3

Discussion

At present, the pathogenesis of RA is considered to be a multifactorial interaction process, and its occurrence and expression are influenced by many risk factors such as heredity and environment [22]. The inflammatory reactions of RA are related to numerous cell types, and FLS have been identified as the cells responsible for and destruction of cartilage and bone. RA is characterized by the proliferation of synoviocytes in inflamed synovia. Moreover, synovial fibroblasts show evidence of transformation indicated by excessive proliferation, loss of contact inhibition and increased migration [23]. Unfortunately, although there are many RA treatment options available, including traditional disease-modifying antirheumatic drugs (DMARDs) and currently available biologicals agents, the general effectiveness of the drugs has been far from satisfaction [24]. Therefore, we should pay more attention to the development of novel drugs for treating RA. Numerous previous reports indicated that the Cinnamomi ramulus extracts (CRE) has a variety of biological actions, including anti-microbial, anti-inflammation, and anti-RA activities. On the basis of the known anti-inflammatory and anti-RA effects of Cinnamomi ramulus, we investigated the effects of Cinnamomi ramulus on RA using human synovial cell line MH7A cells and its underlying mechanisms.

In the present study, CCK-8 assays results showed that Cinnamomi ramulus can significantly inhibit the cell viability and proliferation in a dose-dependent manner, indicating that Cinnamomi ramulus exerts potent anti-proliferative effect on MH7A cells. To investigate the mechanism by which Cinnamomi ramulus inhibits synovial cell proliferation, we evaluated the ability of Cinnamomi ramulus to induce MH7A cells apoptosis and cycle arrest. Promoting programmed cell death (apoptosis) is an important

strategy for RA therapy [25, 26]. It's known that there are two main ways for apoptosis: The death receptor way and the intrinsic mitochondrial way. The intrinsic mitochondrial mediated apoptosis is considered to be the more critical way of the two [27, 28]. Mitochondrial mediated apoptosis is largely regulated by the Bcl-2 protein family. It is well known that the Bcl-2 family proteins, anti-apoptotic proteins such as Bcl-2, inhibit apoptosis, while pro-apoptotic proteins, such as Bax, activate apoptosis in RA [29]. In this study, our results showed that Cinnamomi ramulus increased the expression of Bax in MH7A, as well as decreased the expression of Bcl-2 protein. Moreover, the expressions of cleaved caspases 3 was significantly up-regulated in MH7A cells by Cinnamomi ramulus. These results collectively indicated that Cinnamomi ramulus has obvious pro-apoptotic effect on MH7A cells.

Cell cycle control is the major regulatory mechanism of cell growth, and central to this process are the cyclin-dependent kinases (Cdks), which complex with the cyclin proteins [30]. In G2-M transition, the cyclin-dependent protein kinase complex, CDC2-Cyclin B1 complex could be used as a marker of G2/M phase arrest [31]. P53 protein was a key tumor suppressor in cells. Through downregulating the expression of gene products which are essential for progression through the cell cycle, activation of the P53 tumor suppressor can lead to cell cycle arrest [32]. Furthermore, P21 also act cyclindependent kinase inhibitors able to arrest cells in the G2/M phase [33]. The Cyclin D-CDK4 complex plays a role in G1 phase, and the cell cycle enters G1 phase when CDK4 and CDK6 form active complexes with D-type cyclins. However, a recent study found that CDK4 plays an unexpected role in the G2/M checkpoint [34, 35]. In this study, we detected the distribution of cell cycle of MH7A cells by flow cytometry, and found that Cinnamomi ramulus can significantly increase the proportion of MH7A cells in G2/M phase in a concentration-dependent manner. Therefore, we speculated that Cinnamomi ramulus could induce G2/M phase arrest of MH7A cells. To further verify this hypothesis, Western blotting and q-PCR assays were performed to detect the expression levels of cycle-related proteins. The results showed that Cinnamomi ramulus could reduce the expression of CDC2 and Cyclin B1 in MH7A cells and up-regulate P53, P21 and Cyclin D. In addition, we also found that Cinnamomi ramulus can down-regulate the expression of CDK4. Therefore, Cinnamomi ramulus-induced G2/M blockade may be due to up-regulation of P53, P21 and Cyclin D, and down-regulation of Cyclin B1, CDC2 and CDK4.

Current studies have found that stimulated synovial fibroblasts migrates to intra-articular structures, leading to cartilage and bone damage, which is a major change in the pathogenesis of RA [36]. In the present study, the reduced numbers of transmembrane cells in Transwell chambers and the scratch wound assays showed Cinnamomi ramulus could suppress the migration and invasive capacity of synovial fibroblasts. MMPs, a family of zinc-dependent proteases, are the main proteases for invasion and degradation of basement membranes and extracellular matrix. According to previous study, inhibition of MMPs can significantly reduce cell invasion and migration of synovial fibroblasts [37]. In our study, we found out that Cinnamomi ramulus suppressed MMP-1, -2 & -3 expression concentration-dependently.

Traditional Chinese medicine (TCM) has the characteristics of multiple components and multiple targets, resulting in its unclear basis of medicinal substances and unclear mechanism of action, which seriously

restricts the development and promotion of TCM. In recent years, molecular docking method has become an important technology in the field of computer-aided drug research, which can realize rapid and high-throughput screening of potential drugs and greatly reduce the research and development cost and time [38]. Therefore, more and more researchers have introduced molecular docking into the study of TCMs. In this study, molecular docking results showed that compounds in Cinnamomi ramulus had a good affinity with protein crystals. Notably, the docking fraction of benzyl cinnamate with 9 proteins was higher than that of the prototype ligand, indicating that Benzyl cinnamate may be closely related to the anti-RA effect of Cinnamomi ramulus, and is the main active component of the apoptosis and cycle arrest of synovial fibroblasts induced by Cinnamomi ramulus.

Conclusion

Taken together, these data mentioned above suggested that Cinnamomi ramulus might be beneficial for relieving RA clinic symptoms through induction of apoptosis, cell arrest, and suppression of invasion and migration of synovial fibroblasts.

Abbreviations

RA: rheumatoid arthritis; Bax: Bcl-2-associated X; Bcl: B-cell lymphoma factor; Caspase: Cysteinyl aspartate specific proteinase; ELISA: enzyme-linked immunosorbent assays; MMP: matrix metalloproteinases; NSAIDs: non-steroidal anti-inflammatory drugs; qRT-PCR: real-time fluorescence quantitative PCR; RA: rheumatoid arthritis; TCM: traditional Chinese medicine; CRE: *Cinnamomi ramulus* extract; TNF: tumour necrosis factor.

Declarations

Acknowledgements

Not applicable.

Authors' contributions

JL and QZ designed the study and completed the experimental process, literature search, and generation of figures. JL, QZ, XP and CW wrote and edited the manuscript. RL, SW, YG and JW completed generation of figures. All authors reviewed the manuscript. All authors read and approved the final manuscript.

Funding

This work was supported by the Sichuan Science and Technology Program (grant number 2019JDRC0074), National Science and Technology Major Project of the Ministry of Science and Technology of China (grant number 2018ZX09721004-009-002), and China Postdoctoral Science Foundation (grant number 2018M631071).

Availability of data and materials

Not applicable.

Ethics approval and consent to participate

Not applicable.

Consent for publication

Not applicable.

Competing interests

The authors declare that they have no competing interests.

References

1. Müller-Ladner U, Pap T, Gay RE, Neidhart M, Gay S. Mechanisms of disease: the molecular and cellular basis of joint destruction in rheumatoid arthritis. Nat Clin Pract Rheumatol. 2005;1(2):102–110.
2. Scott DL, Steer S. The course of established rheumatoid arthritis. Best Pract Res Clin Rheumatol. 2007;21(5):943–967.
3. Bustamante MF, Garcia-Carbonell R, Whisenant KD, Guma M. Fibroblast-like synoviocyte metabolism in the pathogenesis of rheumatoid arthritis. Arthritis Res Ther. 2017;19(1):110.
4. Huber LC, Distler O, Tarner I, Gay RE, Gay S, Pap T. Synovial fibroblasts: key players in rheumatoid arthritis. Rheumatology. 2006;45(6):669–675.
5. Malemud CJ. Matrix Metalloproteinases and Synovial Joint Pathology. Prog Mol Biol Transl Sci. 2017;148:305–325.

6. Abeles AM, Pillinger MH. The role of the synovial fibroblast in rheumatoid arthritis: cartilage destruction and the regulation of matrix metalloproteinases. Bull NYU Hosp Jt Dis. 2006;64(1-2):20–24.
7. Kim GJ, Lee JY, Choi HG, Kim SY, Kim E, Shim SH, Nam JW, Kim SH, Choi H. Cinnamomulactone, a new butyrolactone from the twigs of Cinnamomum cassia and its inhibitory activity of matrix metalloproteinases. Arch Pharm Res. 2017;40(3):304–310.
8. Zhang Q, Peng W, Wei S, Wei D, Li R, Liu J, Peng L, Yang S, Gao Y, Wu C, Pu Guizhi-Shaoyao-Zhimu decoction possesses anti-arthritic effects on type II collagen-induced arthritis in rats via suppression of inflammatory reactions, inhibition of invasion & migration and induction of apoptosis in synovial fibroblasts. Biomed Pharmacother. 2019;118:109367.
9. Sun L, Zong SB, Li JC, Lv YZ, Liu LN, Wang ZZ, Zhou J, Cao L, Kou JP, Xiao W. The essential oil from the twigs of Cinnamomum cassia Presl alleviates pain and inflammation in mice. J Ethnopharmacol. 2016;194:904–912.
10. Park GH, Song HM, Park SB, Son HJ, Um Y, Kim HS, J. B. Jeong JB. Cytotoxic activity of the twigs of Cinnamomum cassia through the suppression of cell proliferation and the induction of apoptosis in human colorectal cancer cells. BMC Complement Altern Med. 2018;18(1):28.
11. Liu X, Fu J, Yao XJ, Yang J, Liu L, Xie TG, Jiang PC, Jiang ZH, Zhu GY. Phenolic Constituents Isolated from the Twigs of Cinnamomum cassia and Their Potential Neuroprotective Effects. J Nat Prod. 2018;81(6):1333–1342.
12. Kang JY, Wu Y, Gu WY. Effects of huangqi guizhi wuwu decoction on expression of NLRP3, IL-33 and TGF-β1 in rats with acute gouty arthritis. Journal of Emergency in Traditional Chinese Medicine. 2019;28(11):1989-1992.
13. Zeng CQ, Tan P, Zhang DY, Wu DM, Wu X. Clinical Observation on Treatment of Rheumatoid Arthritis Secondary Osteoporosis with Guizhi Fuzi Decoction and Western Medicine. Chinese Archives of Traditional Chinese Medicine. 2019;37(11):2737-2740.
14. Yang JJ. Analysis on the clinical effect and prognosis of chai hu guizhi ganjiang decoction in the treatment of knee osteoarthritis. Biped and Health. 2019;28(20): 185-186.
15. Franken NA, Rodermond HM, Stap J, Haveman J, van Bree C. Clonogenic assay of cells in vitro. Nat Protoc. 2006;1(5):2315–2319.
16. Araki Y, Mimura T. Matrix Metalloproteinase Gene Activation Resulting from Disordred Epigenetic Mechanisms in Rheumatoid Arthritis. Int J Mol Sci. 2017;18(5):905.
17. Aliboni A, D'Andrea A, Massanisso P. Propolis specimens from different locations of central Italy: chemical profiling and gas chromatography-mass spectrometry (GC-MS) quantitative analysis of the allergenic esters benzyl cinnamate and benzyl salicylate. J Agric Food Chem. 2011;59(1):282–288.
18. Chen PY, Yu JW, Lu FL, Lin MC, Cheng HF. Differentiating parts of Cinnamomum cassia using LC-qTOF-MS in conjunction with principal component analysis. Biomed Chromatogr. 2016;30(9):1449–1457.

19. Yang QX. Study on chemical constituents of cinnamomi cortex. Guangdong Pharmaceutical University, Guangzhou, China. 2017.
20. He Y, Guo YJ, Gao YY. studies on chemical constituents of root of Cichorium intybus. China Journal of Chinese Materia Medica. 2002;27(3):209–210.
21. Son LC, Dai DN, Thang TD, Huyen DD, Ogunwande IA. Study on Cinnamomum oils: compositional pattern of seven species grown in Vietnam. J Oleo Sci. 2014;63(10):1035–1043.
22. Alamanos Y, Drosos AA. Epidemiology of adult rheumatoid arthritis. Autoimmun Rev. 2005;4(3):130–136.
23. Bartok B, Firestein GS. Fibroblast-like synoviocytes: key effector cells in rheumatoid arthritis. Immunol Rev. 2010;233(1):233–255.
24. Gabay C, Hasler P, Kyburz D, So A, Villiger P, Kempis JV, Walker Biological agents in monotherapy for the treatment of rheumatoid arthritis. Swiss Med Wkly. 2014;144:w13950.
25. Liu H, Pope RM. The role of apoptosis in rheumatoid arthritis. Curr Opin Pharmacol. 2003;3(3):317–322.
26. Li H, Wan A. Apoptosis of rheumatoid arthritis fibroblast-like synoviocytes: possible roles of nitric oxide and the thioredoxin 1. Mediators Inflamm. 2013;2013:953462.
27. Stevens M, Oltean S. Modulation of the Apoptosis Gene Bcl-x Function Through Alternative Splicing. Front Genet. 2019;10:804.
28. Yoon JH, Shin JW, Pham TH, Choi YJ, Ryu HW, Oh SR, Oh JW, Yoon DY. Methyl lucidone induces apoptosis and G2/M phase arrest via the PI3K/Akt/NF-κB pathway in ovarian cancer cells. Pharm Biol. 2020;58(1):51–59.
29. Wang J, Zhao Q. Kaempferitrin inhibits proliferation, induces apoptosis, and ameliorates inflammation in human rheumatoid arthritis fibroblast-like synoviocytes. Phytother Res. 2019;33(6):1726–1735.
30. Dalton S. Linking the Cell Cycle to Cell Fate Decisions. Trends Cell Biol. 2015;25(10):592–600.
31. Park M, Chae HD, Yun J, Jung M, Kim YS, Kim SH, Han MH, Shin Constitutive activation of cyclin B1-associated cdc2 kinase overrides p53-mediated G2-M arrest. Cancer Res. 2000;60(3):542–545.
32. Engeland K. Cell cycle arrest through indirect transcriptional repression by p53: I have a DREAM. Cell Death Differ. 2018;25(1):114–132.
33. Li Y, Wang X, Cheng S, Du J, Deng Z, Zhang Y, Liu Q, Gao J, Cheng B, Ling Diosgenin induces G2/M cell cycle arrest and apoptosis in human hepatocellular carcinoma cells. Oncol Rep. 2015;33(2):693–698.
34. Sheppard KE, Pearson RB, Hannan RD. Unexpected role of CDK4 in a G2/M checkpoint. Cell Cycle. 2015;14(9):1351–1352.
35. Brookes S, Gagrica S, Sanij E, Rowe J, Gregory FJ, Hara E, Peters Evidence for a CDK4-dependent checkpoint in a conditional model of cellular senescence. Cell Cycle. 2015;14(8):1164–1173.

36. Bottini N, Firestein GS. Duality of fibroblast-like synoviocytes in RA: passive responders and imprinted aggressors. Nat Rev Rheumatol. 2013;9(1):24–33.
37. Ma JD, Zhou JJ, Zheng DH, Chen LF, Mo YQ, Wei XN, Yang LJ, Dai L. Serum matrix metalloproteinase-3 as a noninvasive biomarker of histological synovitis for diagnosis of rheumatoid arthritis. Mediators Inflamm. 2014;2014:179284.
38. Peng W, Shen H, Lin B, Han P, Li C, Zhang Q, Ye B, Rahman K, Xin H, Qin L, Han T. Docking study and antiosteoporosis effects of a dibenzylbutane lignan isolated from Litsea cubeba targeting Cathepsin K and MEK1. Med Chem Res. 2018;27(9):2062-2070.

Figures

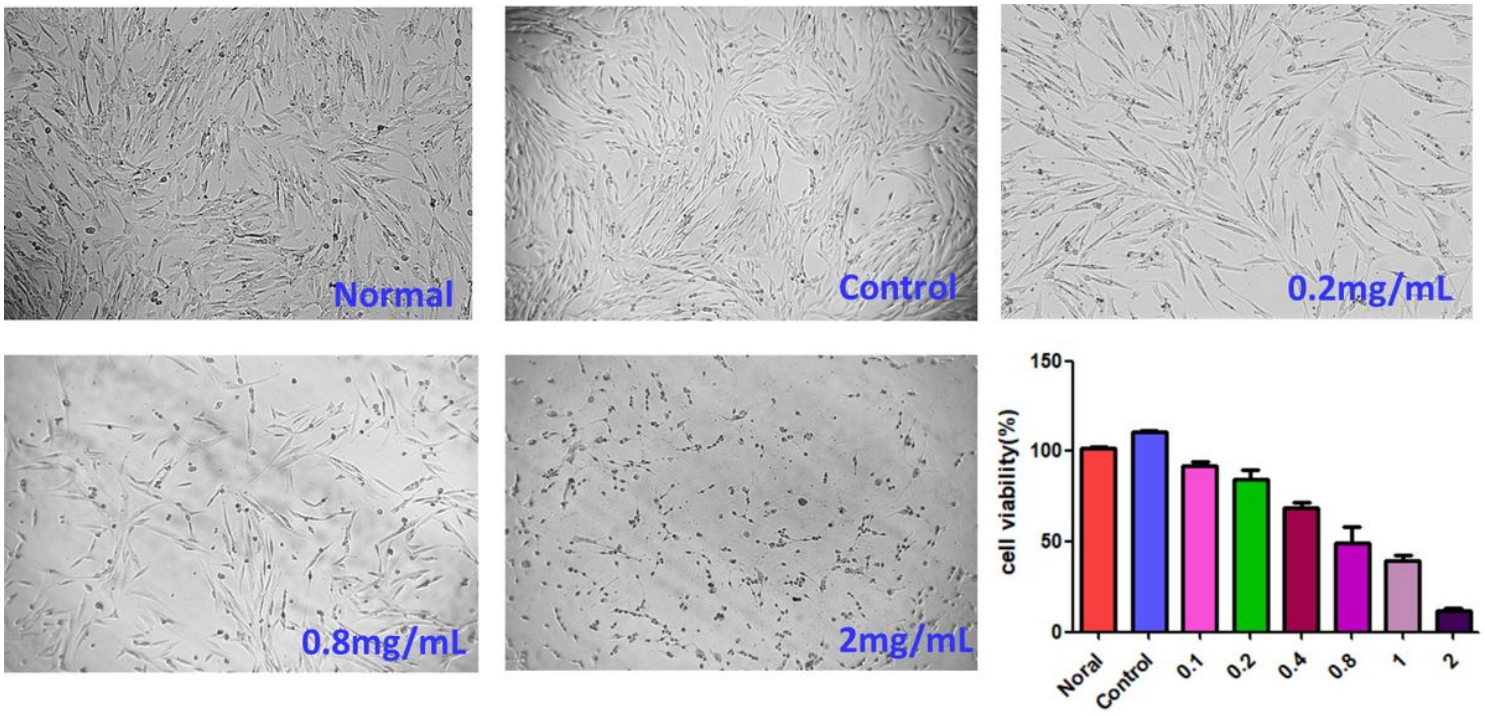

Figure 1

Cytotoxicity of CRE on MH7A cells. MH7A cells were treated with different concentrations of CRE (0.1, 0.2, 0.4, 0.8, 1.0 and 2.0 mg/mL) for 24 h, and cell viability was measured by CCK-8 assay. CRE, Cinnamomi ramulus extracts.

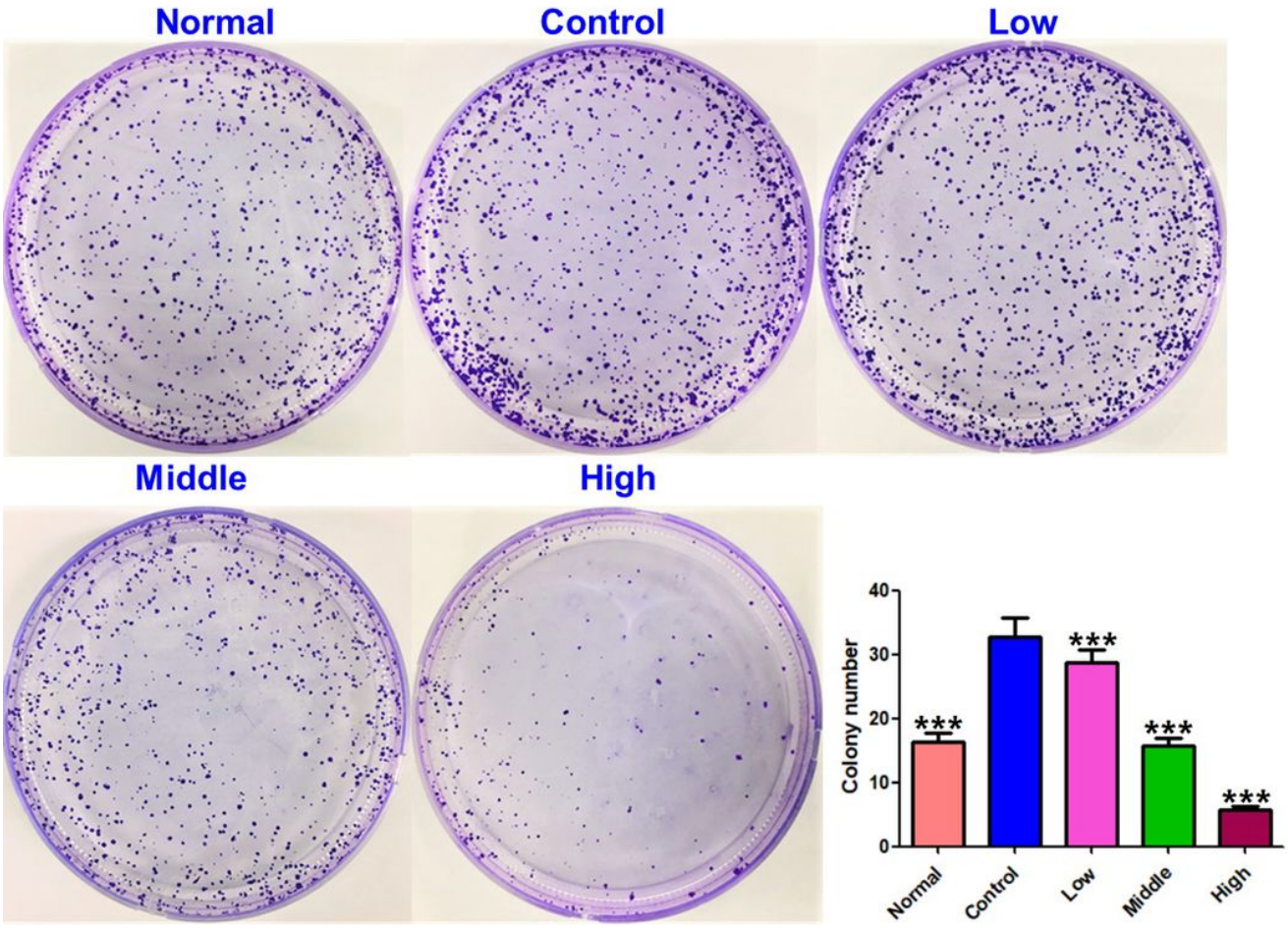

Figure 2

Colony formation assays. Equal numbers of MH7A cells were plated and treated with various concentrations of CRE for 10 days. The number of colony formation was counted in a random microscopic field. Data are expressed as mean ± SD (n = 3), ***P < 0.001, vs. control cells (treated with TNF-α alone). Low, Middle and High concentrations of CRE were 0.2, 0.4, 0.6 mg/mL; CRE, Cinnamomi ramulus extracts.

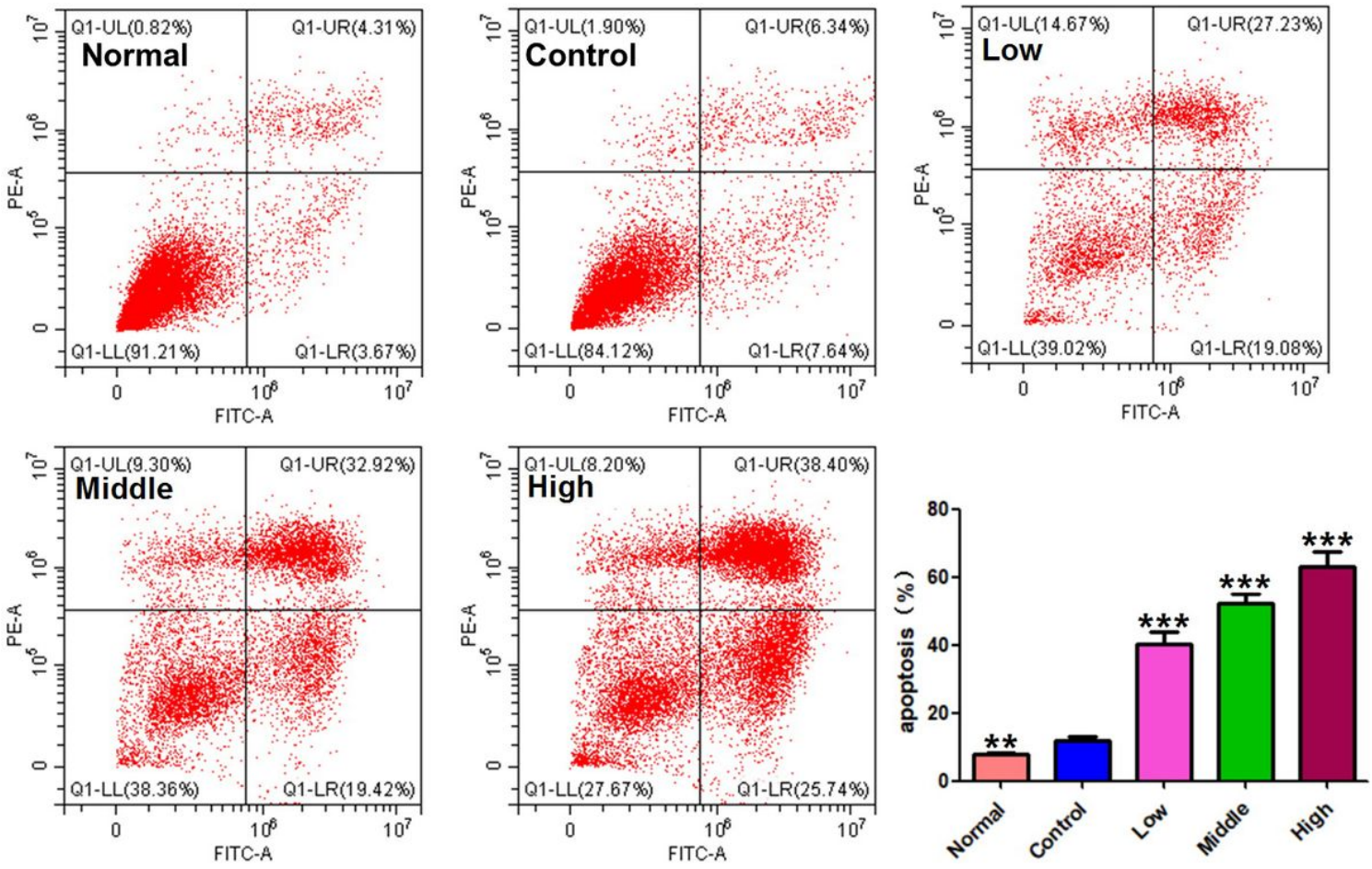

Figure 3

Effect of CRE on apoptosis of MH7A cells. MH7A cells were treated with CRE (0.4, 0.8, 1.2 mg/mL) for 24 h, followed by assessment of apoptosis by flow cytometry analysis. Data are expressed as mean ± SD (n = 3), **P < 0.01, ***P < 0.001, vs. control cells (treated with TNF-α alone). Low, Middle and High concentrations of CRE were 0.4, 0.8, 1.2 mg/mL; CRE, Cinnamomi ramulus extracts.

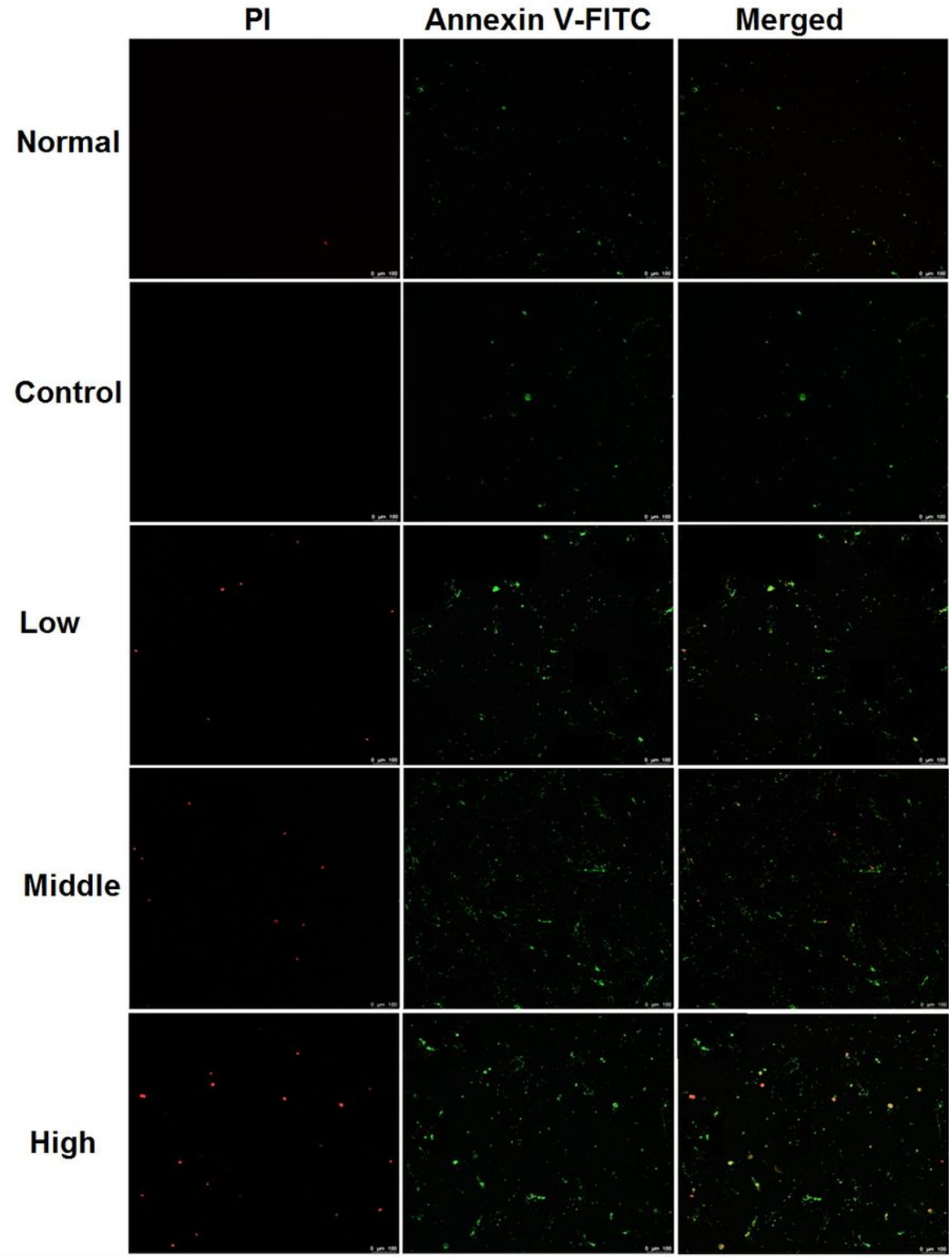

Figure 4

CRE induces apoptosis in MH7A cells. MH7A cells were treated with CRE (0.4, 0.8, 1.2 mg/mL) for 24 h, followed by assessment of apoptosis under laser scanning confocal microscope. Low, Middle and High concentrations of CRE were 0.4, 0.8, 1.2 mg/mL; CRE, Cinnamomi ramulus extracts.

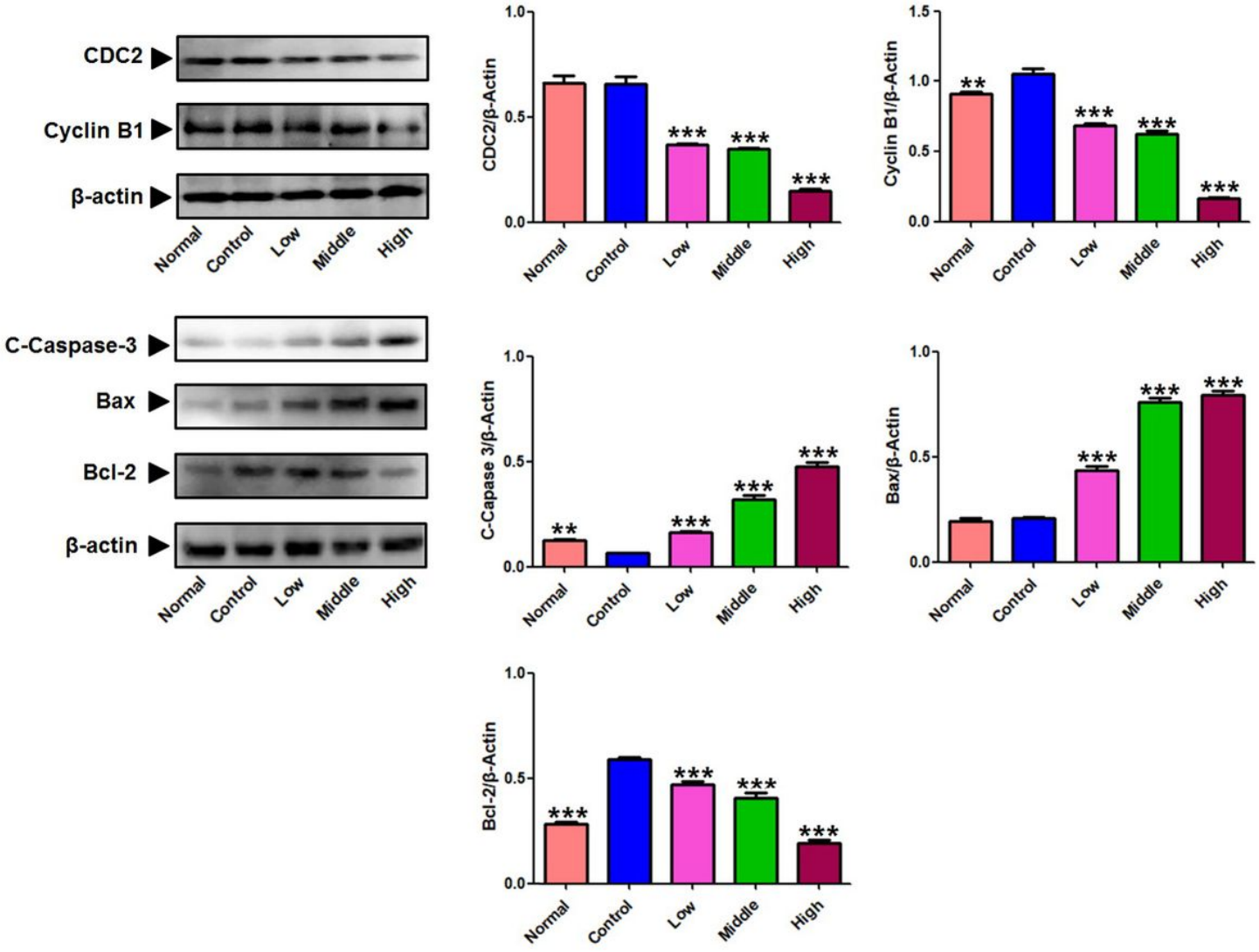

Figure 5

Results of the western blotting assays. Western blot analysis was applied to detect the protein level of C-Caspase-3, Bax, Bcl-2, Cyclin B1 and CDC2 in MH7A treated with CRE (0.2, 0.4, 0.6 mg/mL) for 24 h. β-Actin was used as the sample loading control, Data are expressed as mean ± SD (n = 3), **P < 0.01,***P < 0.001, vs. control cells (treated with TNF-α alone). Low, Middle and High concentrations of CRE were 0.2, 0.4, 0.6 mg/mL; CRE, Cinnamomi ramulus extracts.

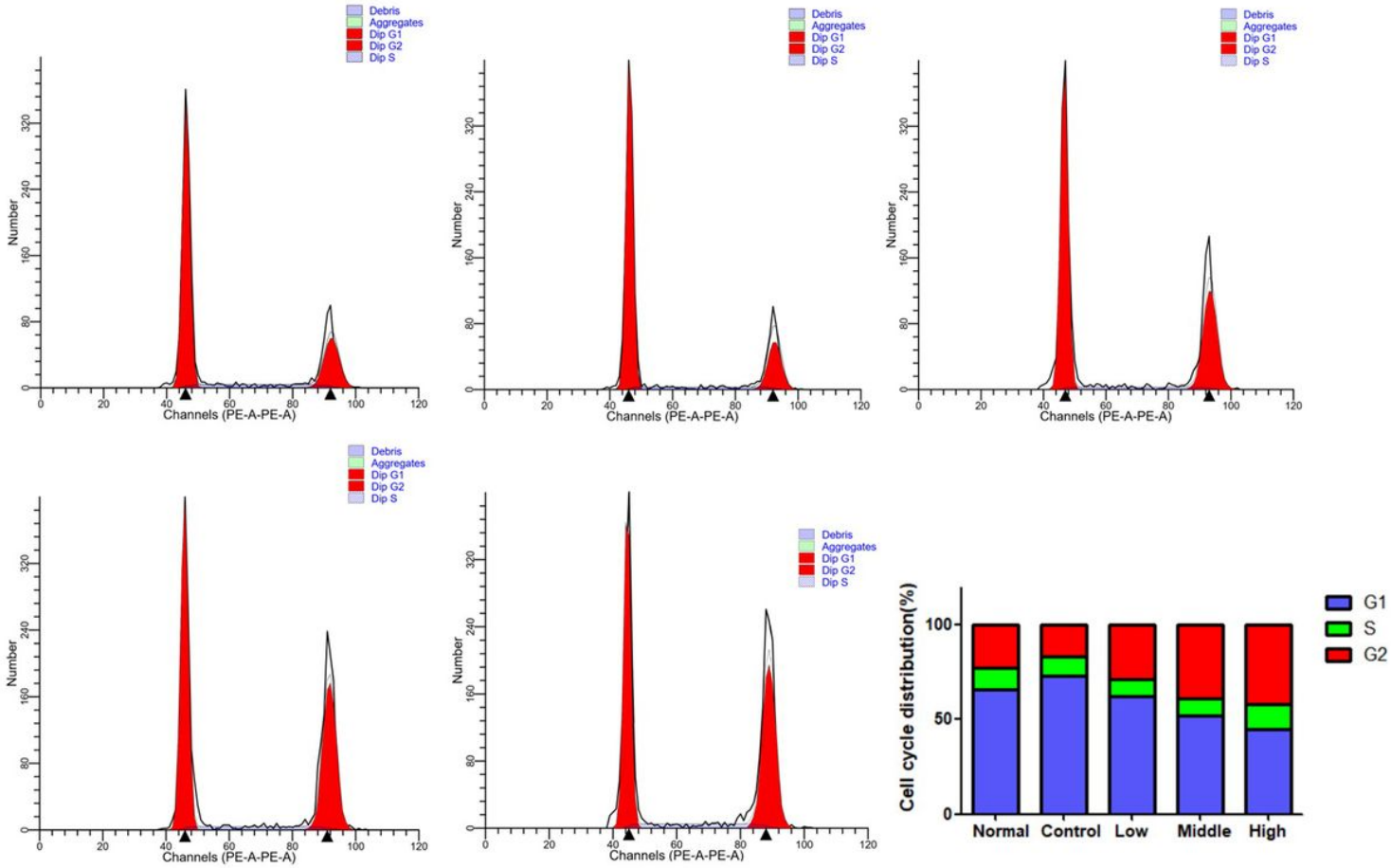

Figure 6

Effect of CRE on the cell cycle in MH7A cells. Flow cytometry was used to assess the cell cycle rate of MH7A cells treated with various concentrations of CRE (0.2, 0.4, 0.6 mg/mL). Histogram represented the statistical analysis of the relative expression level of G2/M related proteins. Data are expressed as mean ± SD (n = 3). Low, Middle and High concentrations of CRE were 0.2, 0.4, 0.6 mg/mL; CRE, Cinnamomi ramulus extracts.

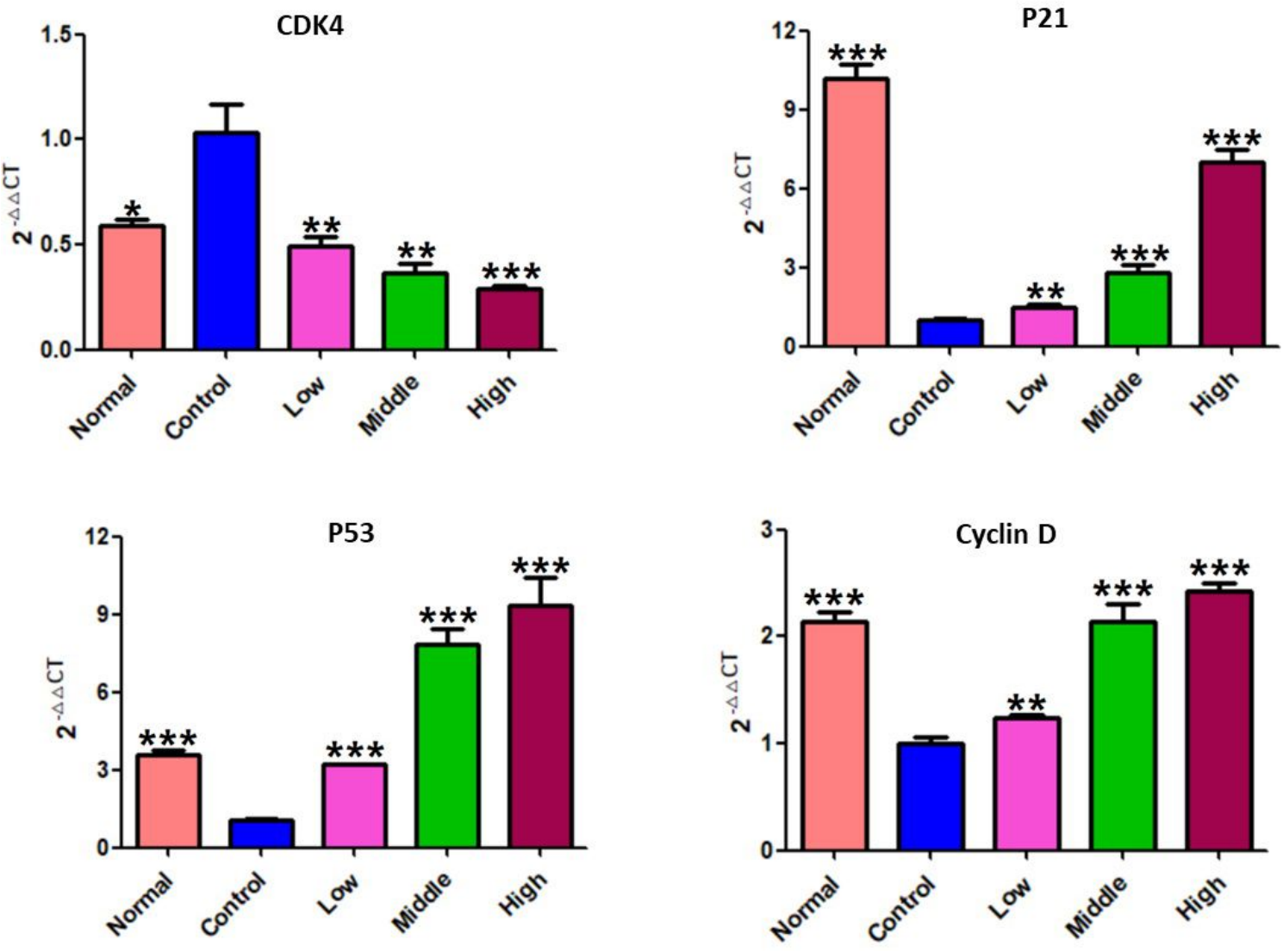

Figure 7

Results of the RT-PCR analysis on P53, P21, CDK4 and CyclinD. Quantitative real-time PCR was performed as described in the Materials and methods. Data are expressed as mean ± SD (n = 3), **P < 0.01,***P < 0.001, vs. control cells (treated with TNF-α alone). Low, Middle and High concentrations of CRE were 0.2, 0.4, 0.6 mg/mL; CRE, Cinnamomi ramulus extracts.

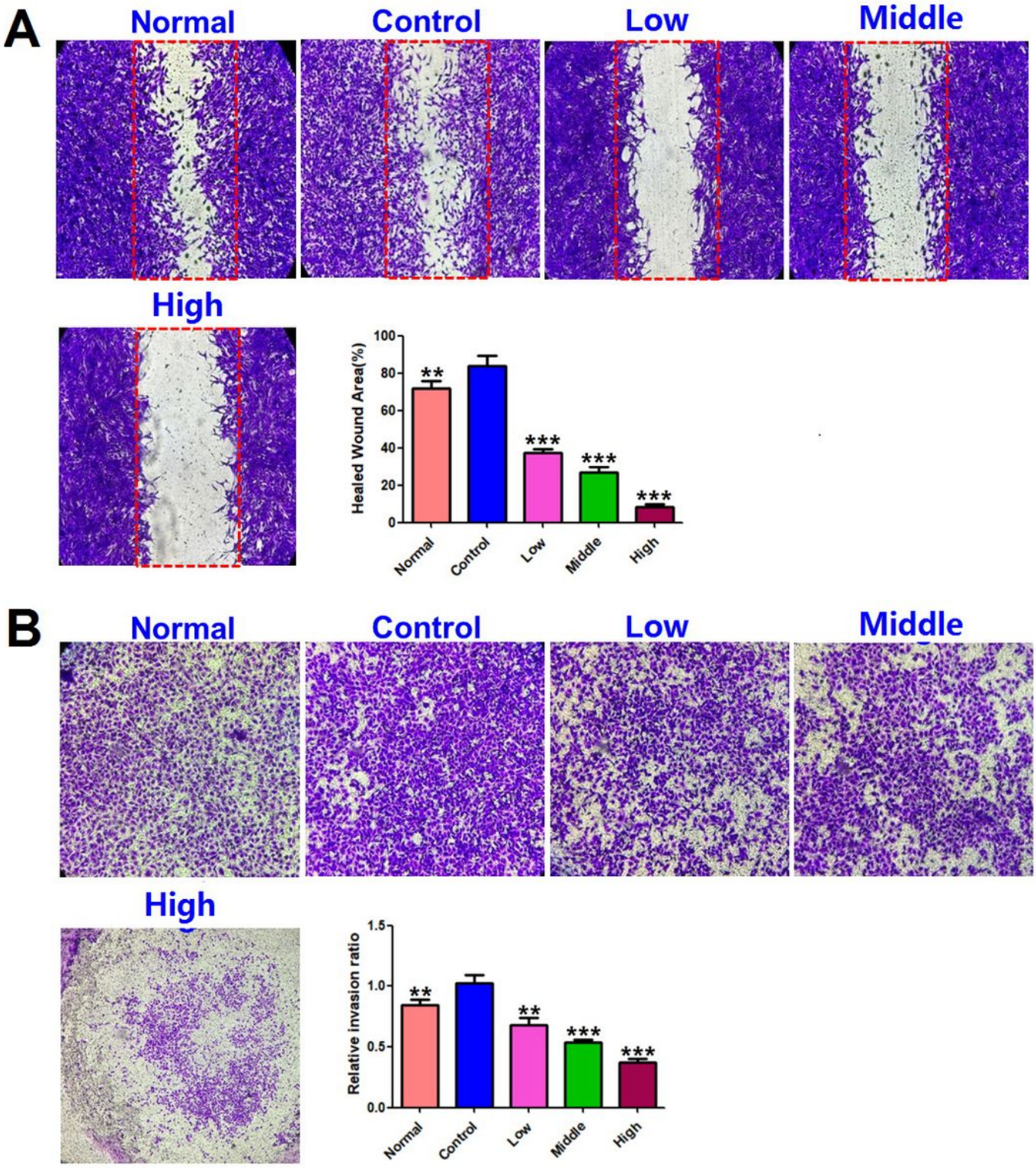

Figure 8

Effects of CRE on migration ability of MH7A cells in wound healing test (A) and transwell migration assay (B) of MH7A cells (200×). Data are expressed as mean ± SD (n = 3), **P < 0.01,***P < 0.001, vs. control cells (treated with TNF-α alone). Low, Middle and High concentrations of CRE were 0.2, 0.4, 0.6 mg/mL; CRE, Cinnamomi ramulus extracts.

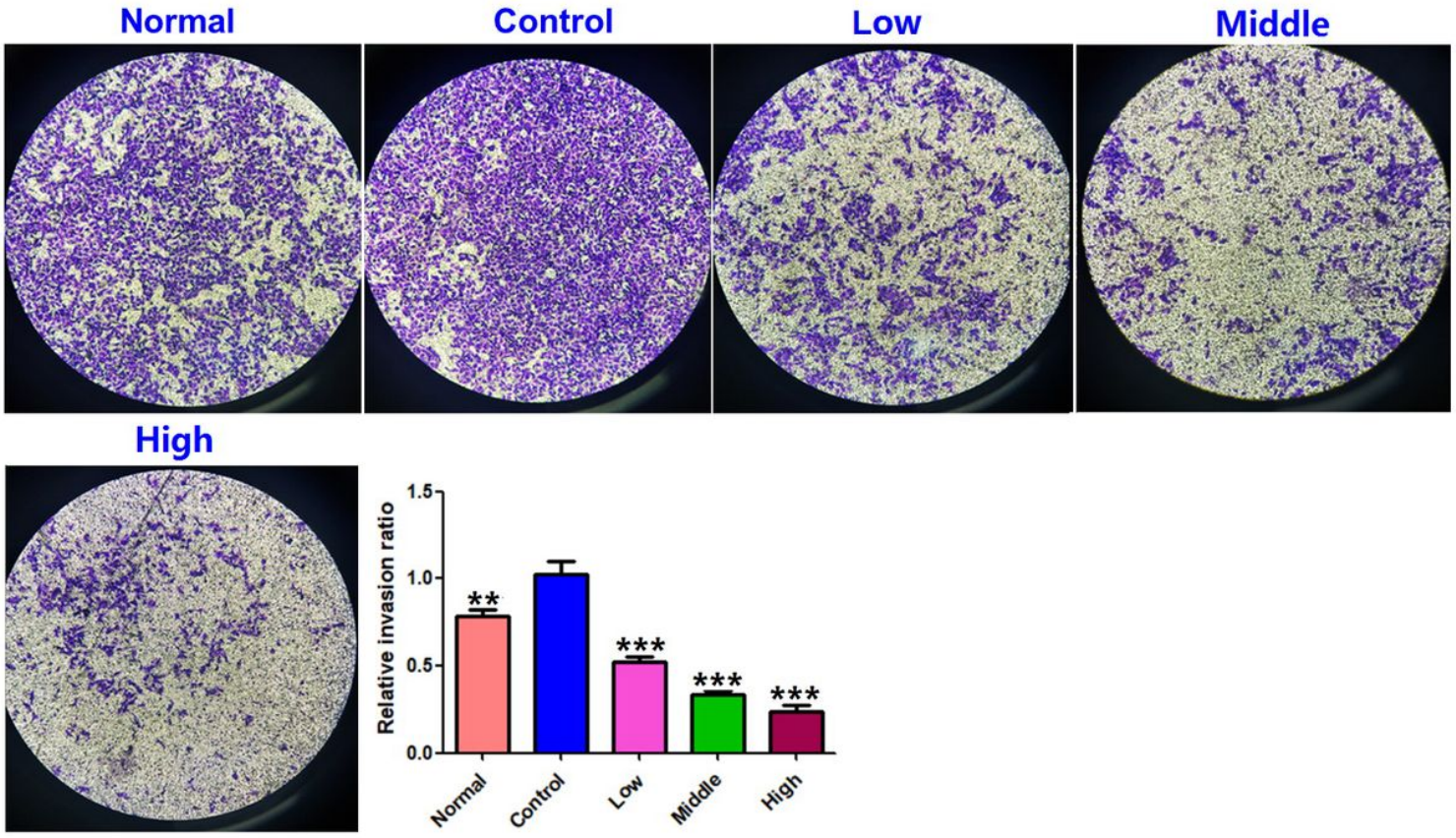

Figure 9

CRE suppresses the invasion ability of MH7A cells. Cell invasion abilities were detected by Matrigel Transwell assay. Cinnamomi ramulus reduced the invasion of MH7A cells in dose-depended manner as demonstrated by representative microscope graphs (200×). Data are expressed as mean ± SD (n = 3), **P < 0.01,***P < 0.001, vs. control cells (treated with TNF-α alone). Low, Middle and High concentrations of CRE were 0.2, 0.4, 0.6 mg/mL; CRE, Cinnamomi ramulus extracts.

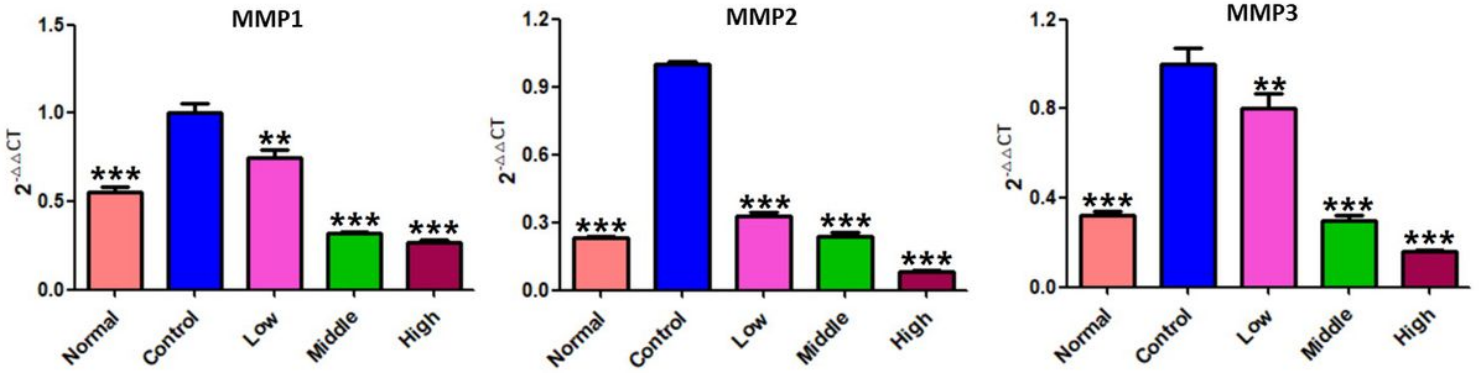

Figure 10

CRE suppresses the expression of MMPs. The mRNA levels of MMP-1, -2 and -3 were determined by using Quantitative real-time PCR (q-PCR). Data are expressed as mean ± SD (n = 3), **P < 0.01,***P < 0.001, vs.

control cells (treated with TNF-α alone). Low, Middle and High concentrations of CRE were 0.2, 0.4, 0.6 mg/mL; CRE, Cinnamomi ramulus extracts.

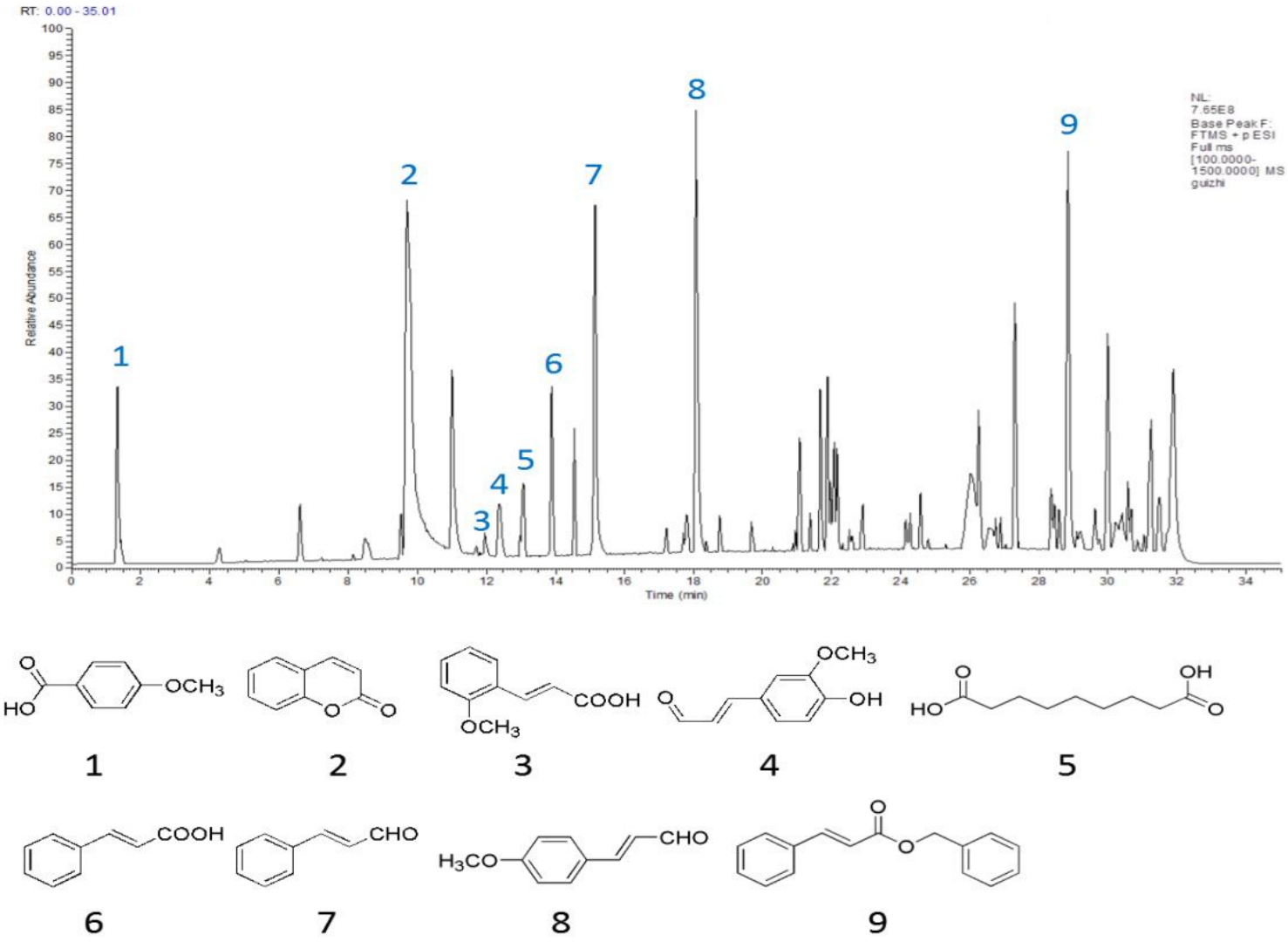

Figure 11

Result of the UPLC-QE-MS/MS assays of the aqueous extracts of Cinnamomi ramulus. The MS total ion chromatograms (TIC) of the crude extract from Cinnamomi ramulus and chemical structures of identified compounds in aqueous extracts of Cinnamomi ramulus.

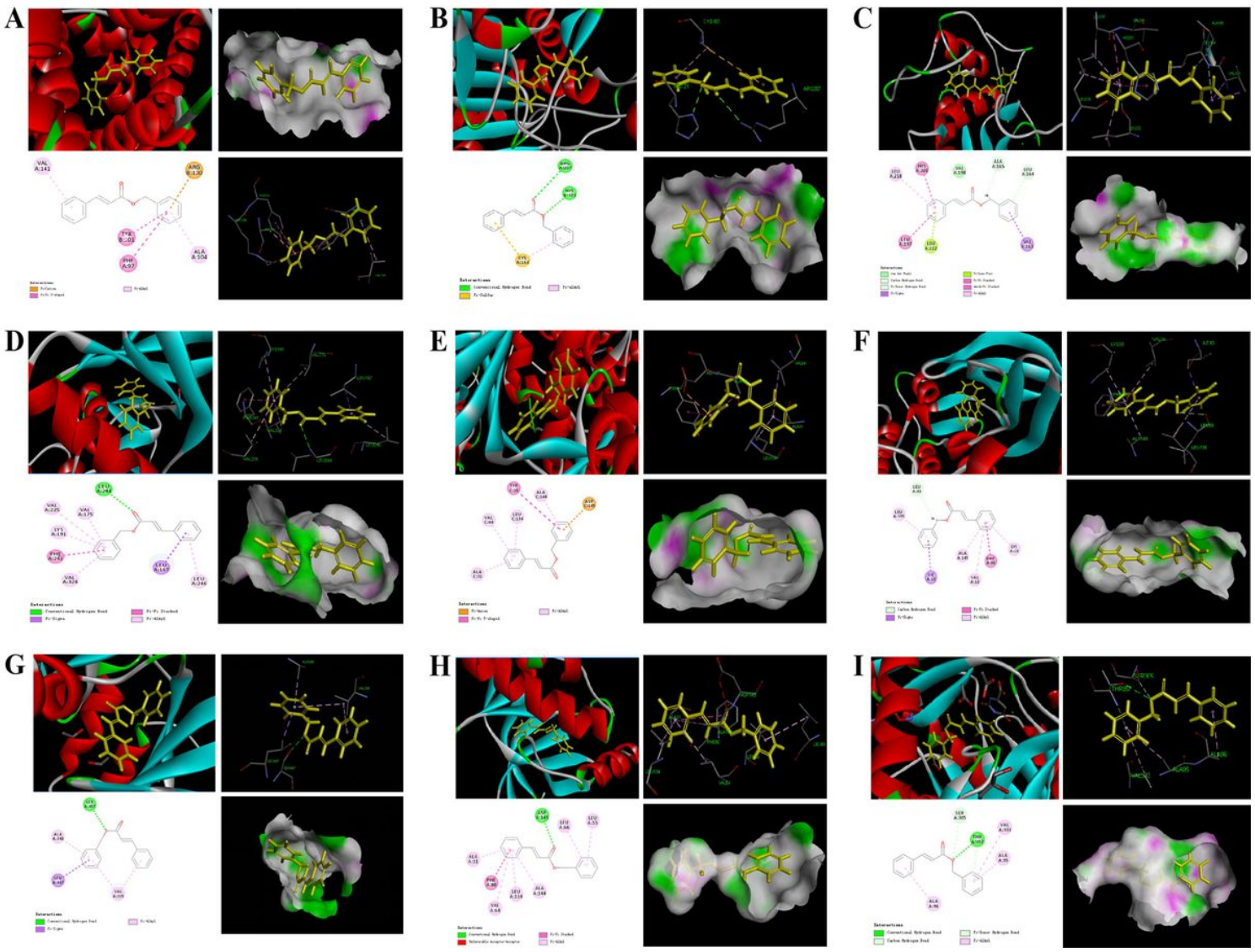

Figure 12

The represented results for the proposed action mode of molecular docking. Molecular docking analyses of benzyl cinnamate (compound 9) to the binding site of human and Bcl-2 (A), caspase 3 (B), MMP3 (C), CDC2 (D), Cyclin D (E), Cyclin B1 (F), P21 (G), CDK4 (H) and P53 (I) proteins.